IIETA International Information and Engineering Technology Association
Advancing the World of Information and Engineering

Mathematical Modelling of Engineering Problems
Vol. 13, No. 1, January, 2026, pp. 119-127
Journal homepage: http://iieta.org/journals/mmep

Comparative Assessment of Displacement-Based Theories for the Static Bending Analysis of Thick Isotropic Beams

Durgesh Tupe[1*], Gajendra Gandhe[1], Satyawan Dhondge[2], Rushikesh Pakhale[3], Changdev Jadhav[3], Arti Wadhekar[4]

[1] Department of Civil Engineering, Deogiri Institute of Engineering and Management Studies, Dr. Babasaheb Ambedkar Technological University, Lonere 431001, India
[2] Department of Science and Humanities, CSMSS Chatrapati Shahu College of Engineering, Dr. Babasaheb Ambedkar Technological University, Lonere 431001, India
[3] Department of Basic Science and Humanities, Deogiri Institute of Engineering and Management Studies, Dr. Babasaheb Ambedkar Technological University, Lonere 431001, India
[4] Department of Electronics and Telecommunication, Deogiri Institute of Engineering and Management Studies, Dr. Babasaheb Ambedkar Technological University, Lonere 431001, India

Corresponding Author Email: durgeshtupe@gmail.com

https://doi.org/10.18280/mmep.130112

Received: 2 September 2025
Revised: 20 December 2025
Accepted: 30 December 2025
Available online: 28 February 2026

Keywords:
thick isotropic beams, shear deformation theory, displacement-based theories, static bending, analytical solution

ABSTRACT

Accurate modeling of thick isotropic beams necessitates the inclusion of transverse shear deformation effects, which are not adequately represented by classical beam theories. In this study, various displacement-based beam theories are evaluated to analyze the static bending behavior of thick isotropic beams. The governing equations are derived using Hamilton's principle through the application of the principle of virtual displacements to satisfy equilibrium conditions. A higher-order shear deformation displacement field is adopted, enabling a realistic representation of shear effects without the need for shear correction factors. Closed-form analytical solutions are obtained by solving the resulting governing equations. The influence of higher-order shear deformation on beam deflection and stress distribution is systematically investigated. Numerical results for isotropic beams subjected to uniformly varying loads are compared with those reported in the existing literature to assess the accuracy of the formulation. The comparisons demonstrate close agreement, thereby confirming the effectiveness and reliability of the present approach. The results clarify the role of higher-order shear deformation effects in the accurate analysis of thick beams and establish the formulation as a robust analytical tool for structural analysis and design applications.

1. INTRODUCTION

The analysis of thick beams continues to pose challenges in structural mechanics due to the significant influence of shear deformation and through-thickness stress variations. Classical beam theory is based on the assumption that beam cross-sections do not warp during bending and remain orthogonal to the neutral axis in the deformed configuration. While this assumption is valid for slender beams, it becomes inaccurate for moderately thick and deep beams where shear effects cannot be neglected. To address these limitations, the first-order shear deformation theory (FSDT), commonly attributed to Timoshenko, introduced a constant transverse shear strain through the thickness. Although FSDT improves accuracy, it requires empirical shear correction factors because the assumption of constant shear distribution is unrealistic for most structural materials. Icardi [1] presented an investigation of laminated and sandwich beams using a unified theoretical framework. Steeves and Fleck [2] considered a failure mechanism in simply supported sandwich beams under three-point bending, advancing a spatial model in comparison with classical beam theories. Magnucka-Blandzi and Magnucki [3] addressed the effective design of a foam-core column under varied loading conditions, focusing on the behavior of the beam under changing constraints. Reddy [4] and Carrera [5] derived equilibrium equations based on generalized theories of support behavior. In his work, both classical and FSDTs were employed to define the governing equilibrium conditions under shear failure hypotheses. Magnucka-Blandzi and Rodak [6, 7] proposed theoretical models for various laminated beams and sandwich beams. They developed a deformation theory that accounts for the displacement of the core relative to the outer faces after bending, and used the principle of minimum total potential energy to derive the equilibrium equations. Morada et al. [8] analyzed the structural reaction of a composite beam under three-point bending. Sayyad and Ghugal [9] provided a comprehensive assessment of numerous experimental studies conducted over the past decade on

composite panels and shells. Findings related to the bending of beams are summarized in this study. Abrate and Scoiva [10] described a classical beam theory based on a single assumption regarding displacement variation across the depth. Paczos et al. [11] presented both analytical and experimental investigations of a novel sandwich-beam configuration under three-point bending; their analytical model was derived using a refined theory. Adámek [12] reviewed and discussed the applicability of the Euler–Bernoulli Theory (ETB) to issues involving laminated beams. Ngoc et al. [13] examined functionally graded curved sandwich beams under buckling, vibration, and bending by applying a higher-order shear deformation theory (HSDT) combined with the Ritz method. Their work derived the governing equations from Lagrange's equations. Ngoc et al. [14] suggested a simpler two-variable shear deformation theory for functionally graded beams, investigating their buckling, bending, and vibration behavior. HSDT reflects shear deformity effects by combining advanced types of in-plane removals or a combination of in-plane and cross-over relocations throughout the joist degree. These theories eliminate the requirement for a shear rectifying element and inherently fulfil the zero-shear pressure state at peak and base side. By analyzing the literature and based on these advanced hypotheses, many dimensions of dependent joist replica have been formulated utilizing overseas flexibility and tension lean theories [15-19]. However, only a limited number of studies have focused on size-dependent higher order linked to the newly proffered global strain ascent validity [20, 21]. Bauchau and Craig [22] formulated the governing equations based on the three fundamental principles of continuum mechanics, kinematic relationships, constitutive laws, and equilibrium conditions. Naumenko and Yang [23] developed a non-local shear deformation beam model using a peridynamic framework to capture long-range interactions. The formulation provides analytical solutions for static and dynamic responses and exhibits clear size-dependent behavior, while recovering classical beam theory results as the non-local length scale diminishes. A second-order beam theory incorporating shear curvature, transverse normal stresses, and rotary inertia was later developed [24]. Ghugal and Shimpi [25] introduced an efficient accordant pure mathematical shear deformation theory to analyze flexural behavior and free vibration in thick beams. Hu et al. [20] demonstrated that the Euler–Bernoulli beam theory is inadequate for accurately describing the response of moderately thick beams because it ignores transverse shear effects. Chitour et al. [19] proposed HSDT-based formulations for evaluating the static behavior of functionally graded beams, using variational techniques to efficiently estimate deflections and stress fields.

This paper critically reviews the existing literature on shear deformation theories applied to the flexural analysis of simply supported beams under static loading, with particular emphasis on the different displacement fields summarized in Table 1. From the literature survey, the following benefits and novelties are revealed. The attainment of analysts in beam investigation served as a trigger for the commitment made in this work. According to the captions, transverse normal strains must be predicted, or else static beam analysis is of no meaning. According to an examination of available research, there is limited literature on the investigation of beams that considers the curvature effect in the shear strain deformation throughout the thickness of a beam. Hence, this study presents an exaggerated shear twisting hypothesis for the examination of a simply supported beam. The most recent versions of the hypothesis focus on working on the shape of the hyperbolic shear deformation hypothesis for beams, including shear deformation and varying thickness. The existing theory provided computational outcomes for transverse displacement, axial displacement, axial stress, and transverse stresses. The achievements of the hypothesis of hyperbolic shear deformation theory (HYSDT) are analyzed in relation to findings from prior research in this field. These limitations motivated the growth of HSDT, which allows the transverse shear strain to vary nonlinearly over the depth and inherently satisfies the zero-shear stress condition at the beam sides. Researchers have proposed refined models for laminated, sandwich, and functionally graded beams. These advancements have significantly improved predictions of bending, vibration, and buckling behaviour in advanced composite structures.

A review of the literature reveals a significant gap in the displacement and stress analysis of isotropic steel beams with varying aspect ratios using shear deformation theories. Although numerous beam models have been developed, most studies focus on laminated composite, sandwich, or functionally graded beams, while research on isotropic beams—particularly using higher-order shear deformation theories—remains limited. In many cases, analyses are restricted to classical or first-order models, leaving the influence of shear strain curvature through the beam thickness insufficiently explored. This limitation is important, as accurate prediction of transverse displacements and stresses is essential in civil, mechanical, defence, and automotive engineering applications where high stiffness and structural reliability are required. Therefore, this study investigates the transverse displacement behavior of isotropic steel beams under various shear deformation theories to address this gap.

The present study addresses this gap by developing and applying a HYSDT for the bending study of simply supported isotropic beams. The proposed theory captures the realistic difference of shear strain without relying on shear correction factors and provides analytical expressions. The governing equations are obtained using Hamilton's principle and resolved to obtain closed-form solutions. To confirm the precision and computational robustness of the proposed model, the outcomes are contrasted with existing theories across different beam aspect ratios.

Table 1. Displacement field of several beam theories available in the literature

Sr. No	Source	Model	Displacement Field
1	Bauchau and Craig [22]	ETB	$f(z) = 0$
2	Naumenko and Yang [23]	FSDT	$f(z) = z$
3	Li et al. [24]	HSDT	$f(z) = z\left[1 - \frac{4}{3}\left(\frac{z^2}{h^2}\right)\right]$
4	Ghugal and Shimpi [25]	TSDT	$f(z) = \frac{h}{\pi} sin\left(\frac{\pi z}{h}\right)$

Note: ETB: Euler–Bernoulli Theory; FSDT: First-order shear deformation theory; HSDT: Higher-order shear deformation theory; TSDT: Trigonometric shear deformation theory

2. MATHEMATICAL FORMULATION AND METHODOLOGY

As shown in Figure 1, the beam analyzed in this work is defined within a three-dimensional Cartesian coordinate framework (x, y, z). The beam extends a length L along the x-axis, has a width b in the y-direction, and a thickness h in the z-direction. The material of the beam is assumed to be uniform, isotropic, and linearly elastic in nature. The material principal directions are aligned with the x- and y-axes lying in the plane of the beam. The stress–strain relationship of the material follows the generalized Hooke's law.

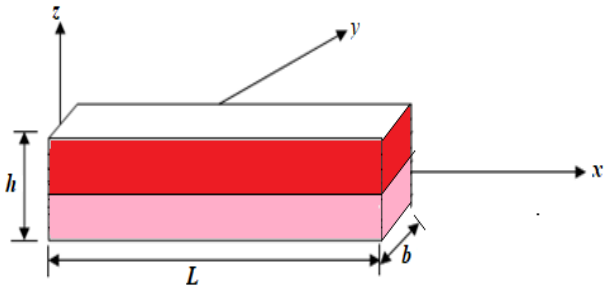

Figure 1. Beam bending in x-z plane

2.1 Assumptions adopted in the conceptual concoction

(1). The axial displacement (u) has two components: one from classical bending theory and another due to shear deformation, assumed hyperboloidal across the thickness with maximum shear stress at the neutral axis.
(2). Axial displacement is defined so that the net in-plane stress (σ_x) produces only bending moments, without generating axial forces.
(3). Transverse displacement (w) depends only on the longitudinal coordinate (x).
(4). Displacements are small compared to the beam thickness.
(5). Effects of body forces are neglected.
(6). A one-dimensional constitutive relation is used.
(7). The beam experiences only lateral loading.

2.2 Displacement field

In accordance with the assumptions stated above, the deformation pattern of the beam illustrated in Figure 2 and the corresponding displacement field of the proposed beam theory are formulated as follows

$$u(x,z) = \frac{3\pi}{2}\left[h\tanh\left(\frac{z}{h}\right) - z\sec^2 h\left(\frac{1}{2}\right)\right]\phi(x)$$
$$w(x,z) = w(x) \tag{1}$$

where,
u = Axial displacement component in the x direction.
w = Transverse displacement in the z direction.
$\phi(x)$ = Unknown function associated with the shear slope.

2.3 Strain-displacement relationships

The normal and shear strain components are attained inside the support of linear elasticity by employing the displacement field defined in Eq. (2). These relationships are given as follows.

Normal strain:

$$\epsilon_x = \frac{\partial u}{\partial x} = -z\frac{\partial^2 w}{\partial x^2} + \frac{3\pi}{2}\left[h\tanh\left(\frac{z}{h}\right) - z\,sec^2\,h\left(\frac{1}{2}\right)\right]\frac{\partial\phi}{\partial x} \tag{2}$$

Shear strain:

$$\gamma_{xz} = \frac{3\pi}{2}\left[\coth\left(\frac{z}{h}\right) - sec^2\,h\left(\frac{1}{2}\right)\right]\phi(x) \tag{3}$$

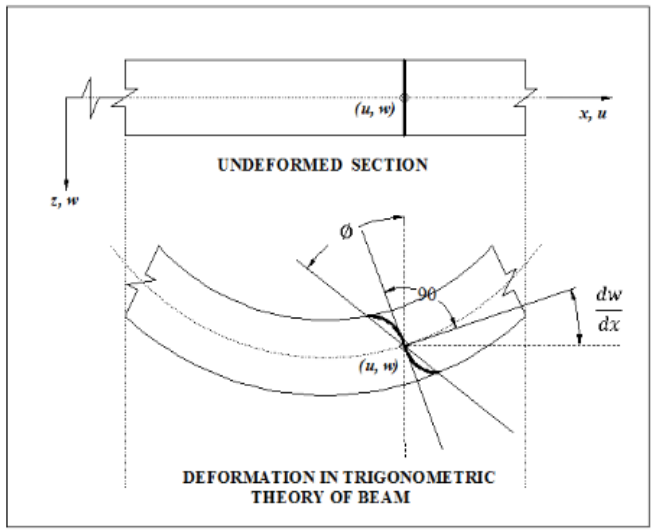

Figure 2. Deformation in hyperbolic shear deformation theory

3. STAIN-DISPLACEMENT RELATIONSHIP

For an isotropic material, the one- dimensional Hooke's law establishes a direct connection between stress and strain. The constitutive equations for normal and shear stresses are expressed:

$$\sigma_x = E\,\epsilon_x = -zE\frac{\partial^2 w}{\partial x^2} + \frac{E3\pi}{2}\left[h\tanh\left(\frac{z}{h}\right) - z\,sec^2\,h\left(\frac{1}{2}\right)\right]\frac{\partial\phi}{\partial x} \tag{4}$$

$$\tau_{xz} = G\gamma_{xz} = G\frac{3\pi}{2}\begin{bmatrix}\coth\left(\frac{z}{h}\right)\\ -\,sec^2\,h\left(\frac{1}{2}\right)\end{bmatrix}\phi(x) \tag{5}$$

The guidelines of virtual work are applicable to beams.

3.1 Governing equations

$$b\int_{x=0}^{x=L}\int_{z=-h/2}^{Z=h/2}(\sigma_x.\,\delta\,\epsilon_x + \tau_{xz}.\,\delta\gamma_{xz})dxdz - \int_{x=0}^{x=L} q\delta w dx = 0 \tag{6}$$

where, δ = Variational operator.

By substituting the expressions for the virtual strains and stresses from Eq. (2) to Eq. (5) into Eq. (6), the following equations are derived. Utilizing Green's hypothesis in Eq. (6)

progressively, the Euler Lagranges's conditions are obtained:

$$EI\left[\frac{\partial^4 w}{\partial x^4} - A_0\frac{\partial^3 \phi}{\partial x^3}\right] = q(x) \tag{7}$$

$$EI\left[A_0\frac{\partial^3 w}{\partial x^3} - B_0\frac{\partial^2 \phi}{\partial x^2}\right] + GAC_0\phi = 0 \tag{8}$$

The stiffness parameters in the governing equations are denoted as A_0, B_0 and C_0. At the boundary, specifically at $x = 0$ and $x = L$ the consistent natural edge states are derived in the following form

$$V_x = EI\left[\frac{\partial^3 w}{\partial x^3} - A_0\frac{\partial^2 \phi}{\partial x^2}\right] = 0 \tag{9}$$

where, w is prescribed.

$$M_x = EI\left[\frac{\partial^2 w}{\partial x^2} - A_0\frac{\partial \phi}{\partial x}\right] = 0 \tag{10}$$

where, $\frac{dw}{dx}$ is prescribed.

$$M_x = EI\left[A_0\frac{\partial^2 w}{\partial x^2} - B_0\frac{\partial \phi}{\partial x}\right] = 0 \tag{11}$$

where, ϕ is prescribed.

According to the basic beam bending theory, the resultant shear force and bending moment are represented by V_x and M_x, respectively.

Eq. (7) and Eq. (8) provide the generic equations for the transverse displacement $w(x)$ and $\phi(x)$ by removing a few terms. Eq. (7) rearranged, and the integration is completed to provide the following equations.

The administering differential conditions were acquired as follows

$$\frac{\partial^3 w}{\partial x^3} = A_0\frac{\partial^2 \phi}{\partial x^2} + \frac{Q(x)}{D} \tag{12}$$

where, the shear force Q (x) is determined by

$$Q(x) = \int_0^x q dx + k_1 \tag{13}$$

Additionally, the following equation is produced by rearranging the second governing Eq. (8).

$$\frac{\partial^3 w}{\partial x^3} = \frac{B_0}{A_0}\frac{\partial^2 \phi}{\partial x^2} - B_0 \tag{14}$$

By placing Eq. (12) second regulating Eq. (14), a single equation in terms of, it gets

$$\alpha\left(\frac{\partial^2 \phi}{\partial x^2}\right) - \beta(\phi) = \frac{Q(x)}{EI} \tag{15}$$

where, the constants are α and β. The auxiliary equation for the general solution of Eq. (14) is provided by

$$(D^2 - \lambda^2)\phi = 0 \tag{16}$$

where, λ is the equation's constant value. The solution to Eq. (16) is divided into two halves, complementary function and particular integral, combining two halves. Yield the complete remedy, which is shown below

$$\phi = k_2\, cosh(\lambda x) + k_3\, sinh(\lambda x) - \left(\frac{Q(x)}{\beta EI}\right) \tag{17}$$

By entering the value of (x) into Eq. (14) and integrating it three times regarding xx, the expression for the transverse displacement $w(x)$ is achieved. Thus, the succeeding is the general formation of the answer for $w(x)$

$$\begin{aligned} EIw(x) = {} & \int\int\int\int\int q dx dx dx dx \\ & + \frac{D}{\lambda^3}\left(\frac{B_0}{A_0}\lambda^2 - \beta\right)(k_2\, sinh\,\lambda x \\ & + k_3\, cosh\,\lambda x) + \frac{k_1 x^3}{6} + k_4\frac{x^2}{2} \\ & + k_5 x + k_6 \end{aligned} \tag{18}$$

The constants of integration k_1, k_2, k_3, k_4, k_5 and k_6 and these find by applying the relevant natural and kinematic boundary conditions for the beam. The stiffness coefficient namely A_0, B_0, C_0 and D_0 are defined as follows

$$A_0 = E\int_{h/2}^{-h/2} z^2 dz,\ B_0 = E\int_{h/2}^{-h/2} zf(z)dz,\ C_0 = E\int_{h/2}^{-h/2} f^2(z)dz$$

$$D_0 = G\int_{h/2}^{-h/2}\left[f'(z)\right]^2 dz \text{ and } \lambda^2 = \frac{\beta}{\alpha}; \beta = \left(\frac{GAD_0}{DB_0}\right); \alpha = \left(\frac{C_0}{B_0} - B_0\right)$$

where,

A_0 is the extensional (axial) stiffness of the cross-section.

B_0 is the axial–bending coupling coefficient.

C_0 is the coupling between the higher-order shear mode $f(z)$ and the plain extension.

D_0 is the bending stiffness.

4. NUMERICAL EXAMPLE

The simply supported beams' material properties and geometric data are as follows:

Modulus of elasticity = E = 210 GPa, Poisson's ratio μ = 0.30 and density of steel = 7800 kg/m^3, length = L, thickness = h, width = b, load intensity = q_0, aspect ratio = (L/h).

The following describes the kinematics and static boundary requirements for simply supported beam bending scenarios, which vary depending on the kind of support.

Simply supported beam conditions imply zero displacement and zero moment at the ends shown in Figure 3.

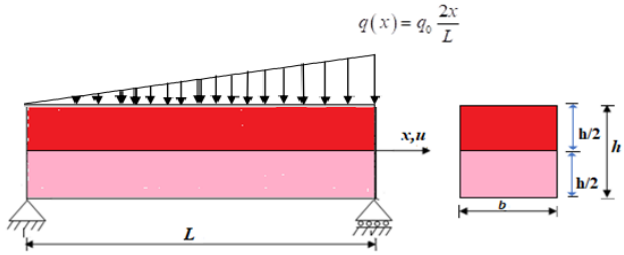

Figure 3. Simply supported beam with linear varying load

At free end: $x = 0$ and $x = L$ (boundary condition)

A simply supported beam with linear varying load, $q(x) = q_0 \frac{2x}{L}$.

Non-dimensional expression for transverse displacement

$$\bar{w}(x)=\left\{\begin{array}{l} 2\frac{x^5}{L^5}-\frac{20x^3}{3L^3}+\frac{14}{3}\frac{x}{L} \\ +20\frac{E}{G}\frac{h^2}{L^2}\frac{A_0^2}{C_0}\left(\frac{\sinh\lambda x}{\lambda^2L^2\cosh\lambda \mathrm{L}}-\frac{1}{\lambda^2L^2}\frac{x}{L}-\frac{x^3}{6L^3}+\frac{1}{6}\frac{x}{L}\right) \end{array}\right\}$$

Non-dimensional expression for axial displacement

$$\bar{u}=-\frac{z}{h}\frac{1}{10}\frac{L^3}{h^3}\left\{\begin{array}{l} \left[\begin{array}{l} 10\frac{x^4}{L^4}-\frac{20x^2}{L^2}+\frac{14}{3} \\ +20\frac{E}{G}\frac{h^2}{L^2}\frac{A_0^2}{C_0}\left(\frac{\cosh\lambda x}{\lambda L\cosh\lambda L}-\frac{1}{\lambda^2L^2}-\frac{1}{2}\frac{x^2}{L^2}+\frac{1}{6}\right) \end{array}\right] \\ +\left[\begin{array}{l} \frac{A_0}{C_0}\frac{E}{G}\frac{L}{h}\frac{3\pi}{2}\left(\tanh\frac{z}{h}-\frac{z}{h}\sec^2h\frac{1}{2}\right) \\ \left(\frac{\cosh\lambda x}{\lambda L\cosh\lambda L}-\frac{1}{\lambda^2L^2}-\frac{1}{2}\frac{x^2}{L^2}+\frac{1}{6}\right) \end{array}\right] \end{array}\right\}$$

Non-dimensional expression for axial stress

$$\bar{\sigma}_x=-\frac{z}{h}\frac{1}{10}\frac{L^2}{h^2}\left\{\begin{array}{l} \left[\begin{array}{l} 40\frac{x^3}{L^3}-\frac{40x}{L} \\ +20\frac{E}{G}\frac{h^2}{L^2}\frac{A_0^2}{C_0}\left(\frac{\sinh\lambda x}{\cosh\lambda L}-\frac{x}{L}\right) \end{array}\right] \\ +\left[\begin{array}{l} \frac{A_0}{C_0}\frac{E}{G}\frac{3\pi}{2}\left(\tanh\frac{z}{h}-\frac{z}{h}\sec^2h\frac{1}{2}\right) \\ \left(\frac{\sinh\lambda x}{\cosh\lambda L}-\frac{x}{L}\right) \end{array}\right] \end{array}\right\}$$

Non-dimensional expression for transverse shear stress using the constitutive relationship

$$\bar{\tau}_{zx}^{CR}=\frac{A_0}{C_0}\frac{L}{h}\left\{\begin{array}{l} \frac{3\pi}{2}\left(\tanh\frac{z}{h}-\frac{z}{h}\sec^2h\frac{1}{2}\right) \\ \left(\frac{\cosh\lambda x}{\lambda L\cosh\lambda L}-\frac{1}{2}\frac{x^2}{L^2}-\frac{1}{\lambda^2L^2}+\frac{1}{6}\right) \end{array}\right\}$$

Non-dimensional expression for transverse shear stress obtained from the equilibrium equation

$$\bar{\tau}_{zx}^{EE}=\frac{1}{80}\frac{L}{h}\left(4\frac{z^2}{h^2}-1\right)\left\{\begin{array}{l} \left[\begin{array}{l} 120\frac{x^2}{L^2}-40 \\ +20\frac{E}{G}\frac{h^2}{L^2}\frac{A_0^2}{C_0}\left(\frac{\lambda L\cosh\lambda x}{\cosh\lambda L}-1\right) \end{array}\right] \\ +\left\{\frac{A_0}{C_0}\frac{E}{G}\frac{h}{L}\frac{3\pi}{2}\right\}\left(\frac{\sinh\lambda x}{\sinh\lambda L}-1\right) \\ \left[\begin{array}{l} \frac{1}{8}\sec^2h\frac{1}{2} \\ \left[\begin{array}{l} \left(1-4\frac{z^2}{h^2}\right) \\ +\log\cosh\frac{z}{h}-\log\cosh\frac{1}{2} \end{array}\right] \end{array}\right] \end{array}\right\}$$

5. RESULTS AND DISCUSSION

For the above loading, the non-dimensional form is

$$\bar{w}=\frac{10wh^3E}{q_0L^4},\ \bar{u}=\frac{buE}{q_0h},\ \bar{\sigma}_x=\frac{b\sigma_x}{q_0},\ \bar{\tau}_{zx}=\frac{b\tau_{zx}}{q_0}$$

Table 2. Comparison of non-dimensional displacements and stresses for simply supported beams (aspect ratios 4 and 10)

Aspect Ratio	Model	Parameter				
		$\bar{u}$	$\bar{w}$	$\bar{\sigma}_x$	$\bar{\tau}_{zx}^{CR}$	$\bar{\tau}_{zx}^{EE}$
4	HYSDT	6.0996	0.616	4.013	1.1613	1.066
	TSDT	5.6913	0.609	3.824	1.0320	0.996
	HSDT	5.6696	0.608	3.815	0.9988	0.995
	FSDT	5.5291	0.608	3.750	1.6000	1.000
	ETB	5.5291	0.532	3.750	-	1.000
10	HYSDT	87.821	0.545	23.70	2.6753	2.561
	TSDT	86.798	0.544	23.51	2.5750	2.498
	HSDT	86.745	0.544	23.50	2.4971	0.998
	FSDT	86.393	0.544	23.43	4.0000	2.450
	ETB	86.393	0.532	23.43	-	2.450

Note: Non-dimensional axial displacement at (x = 0.25 L, z = h/2), transverse displacement at (x = 0.25 L, z = 0.0), axial stress at (x = 0.25 L, z = h/2), maximum transverse shear stress at (x = 0:0, z = h/2) of simply supported beam subjected to varying load for aspect ratio 4 and 10.
HYSDT: Hyperbolic shear deformation theory

Table 2 presents a comparison of the maximum non-dimensional transverse displacement, axial displacement, axial bending stress, and transverse shear stress for beams of aspect ratios 4 and 10 under a uniformly varying load. The percentage error with respect to the EBT is evaluated to quantify the deviation of shear-deformable and higher-order models.

5.1 Displacement behavior

For an aspect ratio of 4, significant discrepancies arise between EBT and shear-deformable models, including the FSDT, TSDT, and HYSDT. This occurs because the EBT assumes zero transverse shear deformation, which is invalid for thick beams. FSDT captures shear effects but requires a shear correction factor, introducing approximation, and TSDT and HYSDT naturally incorporate higher-order shear deformation, producing a more realistic parabolic shear distribution without artificial correction factors. Therefore, higher-order theories predict larger displacement than Euler–Bernoulli because they account for shear flexibility ignored by Euler–Bernoulli. As the aspect ratio increases to 10, the beam

behaves more slenderly; shear strains become negligible. Consequently, the transverse displacement results of HYSDT, TSDT, FSDT, ETB, and Euler–Bernoulli converge, which explains why the percentage error decreases significantly.

5.2 Stress behavior

For an aspect ratio of 4, differences between Euler–Bernoulli and higher-order theories remain small but noticeable because Euler–Bernoulli predicts a purely linear stress distribution, HYSDT and TSDT incorporate nonlinear distribution of displacement fields, especially near surfaces, slightly modifying the stress prediction and FSDT and ETB show similar stress profiles because both rely on first-order kinematics. For an aspect ratio of 10, the bending curvature dominates, and the stress distribution naturally tends toward a linear pattern. Thus, axial stress obtained from all theories aligns closely, resulting in errors of 7% for aspect ratio 4 and 1% or less for aspect ratio 10.

5.3 Transverse shear stress

The most significant differences occur in transverse shear stress, especially for aspect ratio 4, because Euler–Bernoulli predicts zero shear stress—physically incorrect for thick beams, FSDT provides non-zero constant shear stress through the thickness, which still deviates from the actual parabolic form. TSDT and HYSDT inherently satisfy stress-free conditions at the top and bottom surfaces and produce realistic parabolic or higher-order shear profiles. HYSDT, due to its refined higher-order kinematics, gives the most accurate peak location and magnitude. For an aspect ratio of 10, shear stresses are small; therefore, the difference between FSDT, TSDT, and HYSDT becomes minimal, and the influence of higher-order terms diminishes.

Figures 4-12 collectively illustrate the variations of transverse displacement, axial displacement, axial stress, and transverse shear stress for aspect ratios 4 and 10. As shown in Figures 4-12, the transverse displacement (w) is strongly influenced by shear deformation. For aspect ratio 4, higher-order theories predict larger deflection than the Euler–Bernoulli model because they account for shear compliance. For an aspect ratio of 10, all theories converge, indicating that shear effects become negligible in slender beams.

Figures 5 and 6 show that the maximum axial displacement occurs at the top and bottom surfaces of the beam, while the neutral axis remains displacement-free, which agrees with classical bending theory. Differences between the models are more noticeable for aspect ratio 4 due to the additional curvature induced by shear deformation. Figures 7 and 8 demonstrate that axial stress is maximum at the outer surfaces and zero at the neutral axis for all models. For an aspect ratio of 4, higher-order theories slightly alter the peak stress values, whereas for an aspect ratio of 10, these differences become insignificant.

Finally, Figures 9-12 present the transverse shear stress distribution. HYSDT and TSDT naturally satisfy the shear-stress-free boundary conditions and produce realistic parabolic profiles. FSDT requires a shear correction factor and therefore shows slight deviation. The EBT predicts zero shear stress and cannot represent thick-beam behavior. For an aspect ratio of 10, the differences among all shear-deformation theories diminish as shear effects reduce with increasing slenderness.

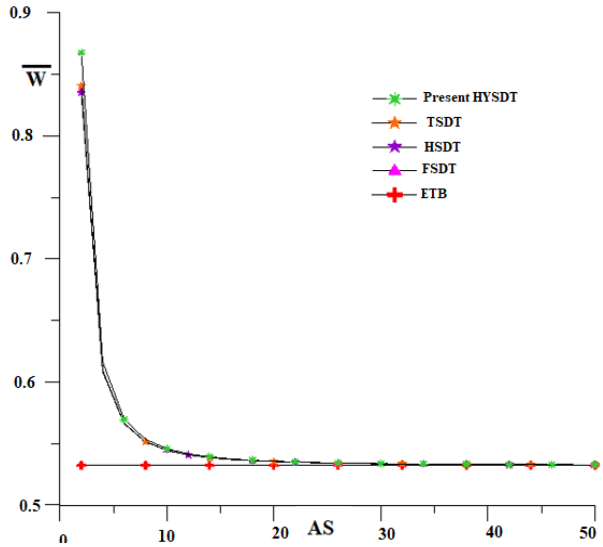

Figure 4. The change in the maximum transverse displacement of a simply supported beam with a different aspect ratio

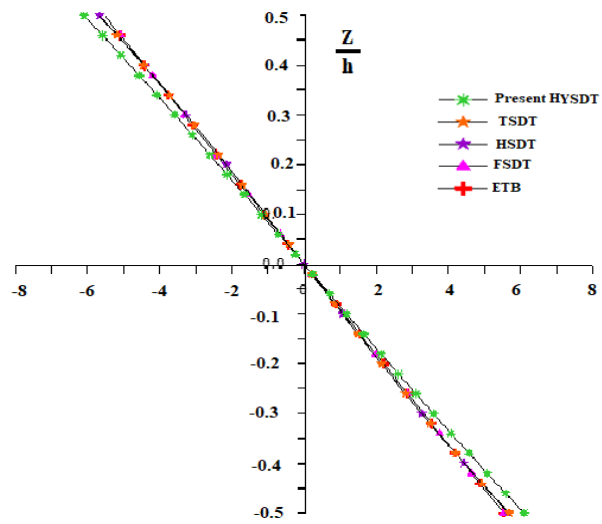

Figure 5. The change of maximum axial displacement with the aspect ratio of 4

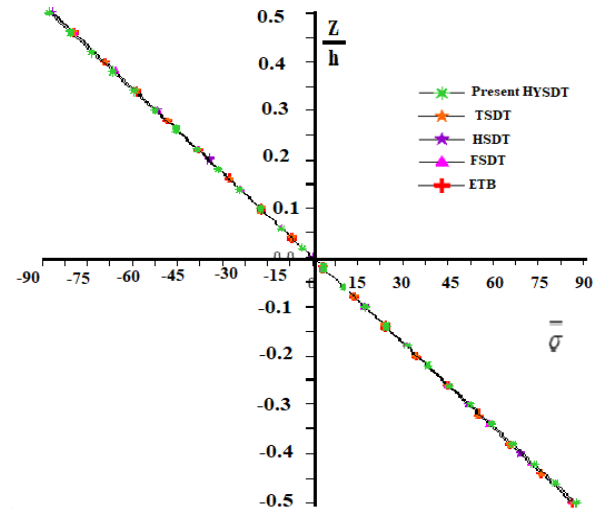

Figure 6. The change of maximum axial displacement with the aspect ratio of 10

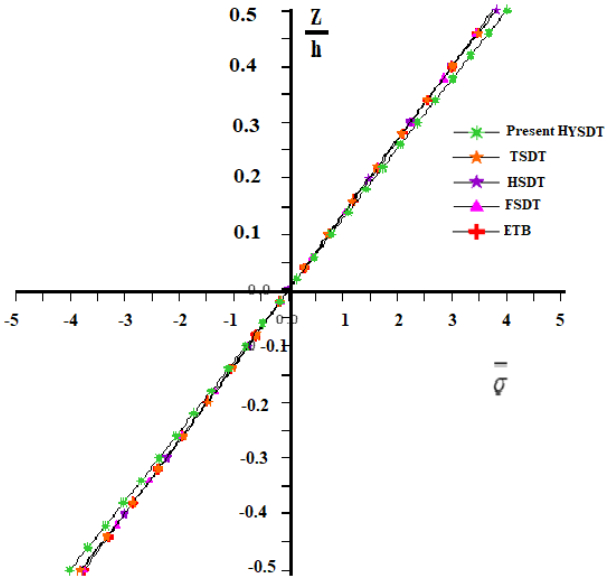

Figure 7. The change of maximum axial stress with the aspect ratio of 4

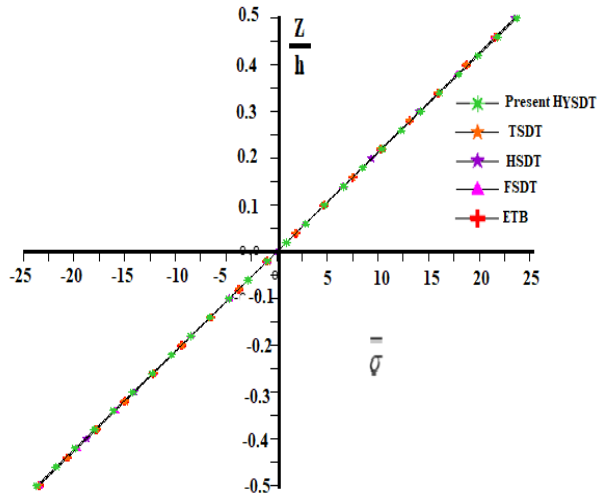

Figure 8. The change of maximum axial stress with the aspect ratio of 10

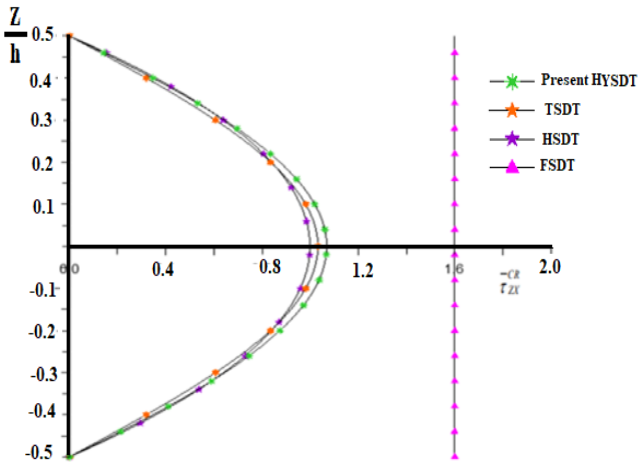

Figure 9. The change of transverse shear stress using the constitutive relation for the aspect ratio of 4

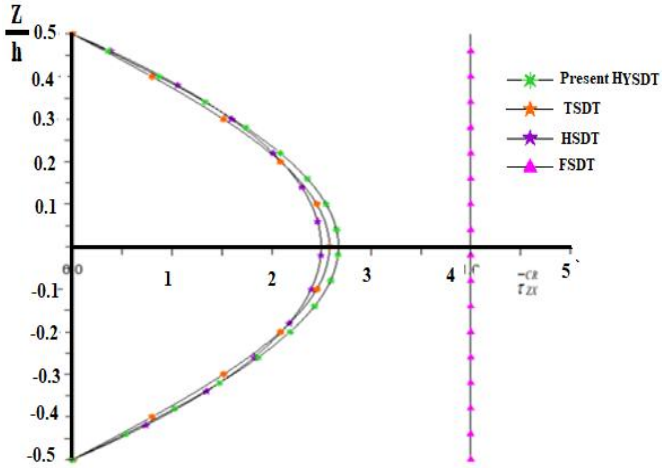

Figure 10. The change of transverse shear using the constitutive relation for the aspect ratio of 10

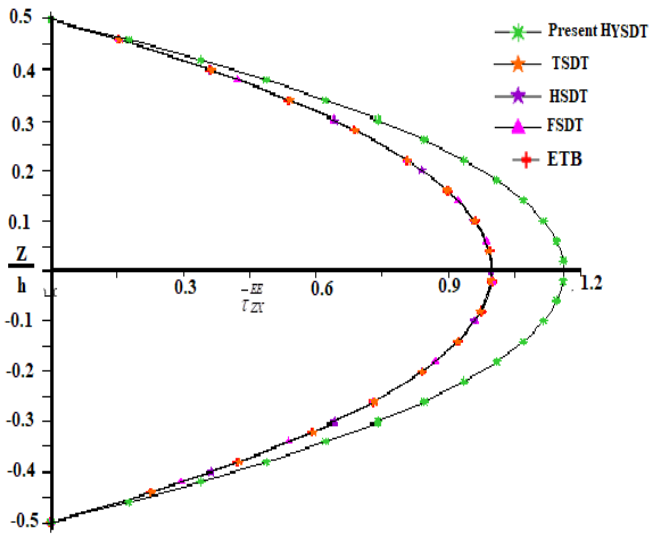

Figure 11. The change of transverse shear stress using the equilibrium equation for the aspect ratio of 4

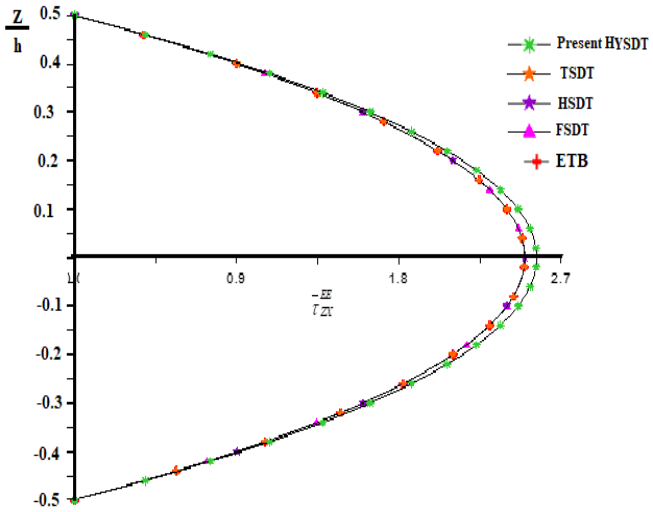

Figure 12. The change of transverse shear stress using the equilibrium equation for the aspect ratio of 10

6. CONCLUSIONS

The present study introduces and evaluates an HYSDT for the bending analysis of thick isotropic beams. The results clearly demonstrate that the proposed HYSDT provides superior accuracy in predicting transverse and axial displacements, bending stresses, and shear stresses when compared with classical ETB, FSDT, and HSDT. The improvement is particularly significant for low aspect ratios, where shear deformation effects dominate, and classical formulations become inadequate. A key strength of the current theory is its ability to satisfy shear-stress-free boundary conditions naturally, without relying on shear correction factors. This leads to a more realistic through-thickness variation of transverse shear stress and eliminates the limitations commonly associated with FSDT-type models. In addition, the two-dimensional equilibrium formulation enables the theory to accurately capture stress concentrations and provide physically consistent stress distributions throughout the beam depth. From a practical standpoint, the enhanced predictive capability of HYSDT makes it especially suitable for the design and analysis of thick structural elements used in aerospace, mechanical, and civil engineering applications such as aircraft wing ribs, turbine blades, machine components, and short-span bridge elements, where shear effects cannot be neglected.

Future work may extend the present formulation to a wider range of applications. Potential research directions include:

(a) Modeling dynamic responses, such as free vibration, impact, and transient loading,
(b) Extending the theory to composite or functionally graded materials with complex anisotropic behavior
(c) Developing finite element implementations for large-scale structural analysis,
(d) Incorporating geometric nonlinearity and stability effects for high-performance structural components, etc.

ACKNOWLEDGMENT

The authors acknowledge the continuous support and encouragement from the Deogiri Institute of Engineering and Management Studies, Chhatrapati Sambhajinagar, Maharashtra State, India.

REFERENCES

[1] Icardi, U. (2003). Applications of Zig-Zag theories to sandwich beams. Mechanics of Advanced Materials and Structures, 10(1): 77-97. https://doi.org/10.1080/15376490306737

[2] Steeves, C.A., Fleck, N.A. (2004). Collapse mechanisms of sandwich beams with composite faces and a foam core, loaded in three-point bending. Part I: Analytical models and minimum weight design. International Journal of Mechanical Sciences, 46(4): 561-583. https://doi.org/10.1016/j.ijmecsci.2004.04.003

[3] Magnucka-Blandzi, E., Magnucki, K. (2007). Effective design of a sandwich beam with a metal foam core. Thin-Walled Structures, 45(4): 432-438. https://doi.org/10.1016/j.tws.2007.03.005

[4] Reddy, J.N. (2010). Nonlocal nonlinear formulations for bending of classical and shear deformation theories of beams and plates. International Journal of Engineering Sciences, 48(11): 1507-1518. https://doi.org/10.1016/j.ijengsci.2010.09.020

[5] Carrera, E. (2003). Historical review of Zig-Zag theories for multilayered plates and shells. Applied Mechanics Reviews, 56(3): 287-308. https://doi.org/10.1115/1.1557614

[6] Magnucka-Blandzi, E., Rodak, M. (2017). Bending and buckling of a metal seven-layer beam with lengthwise corrugated main core–Comparative analysis with sandwich beam. Journal of Theoretical and Applied Mechanics, 55(1): 41-53. http://doi.org/10.15632/jtam-pl.55.1.41

[7] Magnucka-Blandzi, E. (2018). Bending and buckling of a metal seven-layer beam with crosswise corrugated main core–Comparative analysis with sandwich beam. Composite Structures, 183: 35-41. https://doi.org/10.1016/j.compstruct.2016.11.089

[8] Morada, G., Vadean, A., Boukhili, R. (2018). Failure mechanism of a sandwich beam with an epoxy core under static and dynamic three-point bending. Composite Structures, 176: 281-293. https://doi.org/10.1016/j.compstruct.2017.05.023

[9] Sayyad, A.S., Ghugal, Y.M. (2017). Bending, buckling and free vibration of laminated composite and sandwich beams: A critical review of literature. Composite Structures, 171: 486-504. https://doi.org/10.1016/j.compstruct.2017.03.053

[10] Abrate, S., Scoiva, M. (2017). Equivalent single layer theories for composite and sandwich structures: A review. Composite Structures, 179: 482-494. https://doi.org/10.1016/j.compstruct.2017.07.090

[11] Paczos, P., Wichniarek, R., Magnucki, K. (2018). Three-point bending of the sandwich beam with special structures of the core. Composite Structures, 201: 676-682. https://doi.org/10.1016/j.compstruct.2018.06.077

[12] Adámek, V. (2018). The limits of Timoshenko beam theory applied to impact problems of layered beams. International Journal of Mechanical, 145: 128-137. https://doi.org/10.1016/j.ijmecsci.2018.07.001

[13] Ngoc, N., Van, B., Thuc, P. (2025). Higher-order shear deformation theory and Ritz method for analysis of functionally graded sandwich curved beams. Mechanics of Advanced Materials and Structures, 33(1): 1-18. https://doi.org/10.1080/15376494.2025.2524709

[14] Ngoc, N., Van, Thien, N., Thuc, P., Trung, P. (2022). A new two-variable shear deformation theory for bending, free vibration and buckling analysis of functionally graded porous beams. Composite Structures, 282: 115095. https://doi.org/10.1016/j.compstruct.2021.115095

[15] Ntaflos, K.I., Beltsios, K.G., Hadjigeorgiou, E.P. (2024). A unified shear deformation theory for piezoelectric beams with geometric nonlinearities—analytical modelling and bending analysis. Journal of Composites Science, 8(12): 494. https://doi.org/10.3390/jcs8120494

[16] Firouzi, N., Alzaidi, A.S.M. (2024). Non-linear elastic beam deformations with four-parameter Timoshenko beam element considering through-the-thickness stretch parameter and reduced integration. Symmetry, 16(8): 984. https://doi.org/10.3390/sym16080984

[17] Valencia Murillo, C.E., Gutierrez Rivera, M.E., Celaya Garcia, L.D. (2023). Thermal–structural linear static

analysis of functionally graded beams using reddy beam theory. Mathematical and Computational Applications, 28(4): 84. https://doi.org/10.3390/mca28040084

[18] Ali, R., Hirde, S.K. (2024). Flexural analysis of isotropic rectangular beam subjected to uniformly varying load using seventh order shear deformation theory for different boundary conditions. SSRG International Journal of Civil Engineering, 11(9): 61-79. https://doi.org/10.14445/23488352/IJCE-V11I9P106

[19] Chitour, M., Khadraoui, F., Mansouri, K., Rebai, B., Menasria, A., Zemmouri, A., Touati, S., Boumediri, H. (2024). A novel high order theory for static bending of functionally graded (FG) beams subjected to various mechanical loads. Research on Engineering Structures and Materials, 10(4): 1523-1539. http://doi.org/10.17515/resm2024.141me0104rs

[20] Hu, W.F., Liu, Z.H., Cai, S.S., Wang, Y.H., Liu, T., Chen, W.Q. (2025). A higher-order shear deformation theory considering thickness stretching for isotropic plane beams. Engineering Structures, 330: 119887. https://doi.org/10.1016/j.engstruct.2025.119887

[21] Indronil, D. (2025). Sinusoidal shear deformable beam theory for analytic nonlocal elasticity. Partial Differential Equations in Applied Mathematics, 13: 101116. https://doi.org/10.1016/j.padiff.2025.101116

[22] Bauchau, O.A., Craig, J.I. (2009). Euler-Bernoulli beam theory. In Structural Analysis, pp. 173-221. https://doi.org/10.1007/978-90-481-2516-6_5

[23] Naumenko, K., Yang, Z. (2025). First order shear deformation beam theories in a peridynamic framework. European Journal of Mechanics-A/Solids, 112: 105633. https://doi.org/10.1016/j.euromechsol.2025.105633

[24] Li, Y., Liao, Y., Xie, Z., Peng, L. (2024). Stability analysis of curved beams based on first-order shear deformation theory and moving least-squares approximation. Buildings, 14(12): 3887. https://doi.org/10.3390/buildings14123887

[25] Ghugal, Y.M., Shimpi, R.P. (2000). A trigonometric shear deformation theory for flexure and free vibration of isotropic thick beams. In Structural Engineering Convention, SEC-2000, IIT Bombay, India, pp. 255-263.

NOMENCLATURE

A	Cross sectional area of beam
b	Width of beam in y direction
E, G, μ	Elastic constants of the material
Nu	Young's Modulus
G	Shear Modulus
h	Thickness of beam
I	Moment of inertia of beam
L	Span of the beam
q	Intensity of uniformly distributed transverse load
w	Transverse displacement in z direction
EBT	Euler–Bernoulli Theory
FSDT	First-order shear deformation theory
HSDT	Higher-order shear deformation theory
TSDT	Trigonometric shear deformation theory
HYSDT	Hyperbolic shear deformation theory